

A Discontinuous Galerkin Method for the Two-Fluid Plasma Model

John Loverich and Uri Shumlak

University of Washington
Department of Aeronautics and Astronautics

Conference on Computational Physics
Genoa, Italy, September 1-4, 2004

URL <http://www.aa.washington.edu/cfdlab>
email: jlovric@u.washington.edu

ELIGIBLE

Abstract

A discontinuous Galerkin method for the two-fluid plasma model is described. The model includes complete electron and ion fluids, which allows charge separation, separate electron and ion temperatures and velocities. Complete Maxwell's equations are used including displacement current. The algorithm is benchmarked against existing plasma algorithms on the GEM Challenge magnetic reconnection problem. A theta-pinch equilibrium is simulated which generates electron turbulence from an electron current layer. The algorithm can be easily extended to three dimensions, higher order accuracy and general geometries.

Introduction

Plasma physics continues to be an important area of numerical and experimental research. A number of magnetic confinement fusion concepts including tokamaks, spheromaks, FRCs, Z-pinchs and inertial confinement concepts such as pellet implosion are under investigation at various facilities. Further applications include space propulsion, plasma sails, ion thrusters and Hall thrusters. Numerical methods have focused on short time scale small length scale effect with particle codes, or long time scale large spatial effects with MHD (Magnetohydrodynamics) codes[16]. In the process of moving from particle codes to MHD codes[9] a number of intermediate time and spatial scale effects are lost. Recent research has been focused on bridging this gap by using more accurate fluid models including multi-temperature MHD, Hall MHD[3, 4, 12, 1, 13], quasi-neutral two-fluid MHD[11], and the two-fluid model[15] for which only a 1D algorithm has been published. In this paper we develop a discontinuous Galerkin (DG) method for the two-fluid plasma model and show preliminary results in 2D.

Introduction

The MHD equations are an asymptotic limit of the two-fluid plasma model. As such, the two-fluid plasma model describes significantly more physics than the MHD model. This additional physics includes,

- Fast waves - electron plasma waves, R, L, X, O and whistler mode waves.
- Collisionless reconnection, electron Kelvin Helmholtz instabilities.
- Multi-temperature and finite Larmor radius effects.
- Charge separation and Hall currents.
- Separate electron and ion shocks.

This additional physics is useful in modeling non-ideal effects such as two-fluid stability in FRC's[14], and finite Larmor radius effects in Z-pinches and Spheromaks...

Two-Fluid Model

The two-fluid plasma equations are non-dimensionalized as in [15] leaving four non-dimensional parameters. In the following, x_0 is the characteristic plasma size (size of the domain), λ_d is a characteristic Debye length, r_{gi} is a characteristic ion Larmor radius, v_{thi} is the characteristic ion thermal velocity and m_i , and m_e are non-dimensional electron and ion masses where we take $m_i = 1$. The parameters are $\frac{\lambda_d}{x_0}$, $\frac{r_{gi}}{x_0}$, $\frac{v_{thi}}{c}$ and $\frac{m_i}{m_e}$. In all cases ions are singly charged. In the equations that follow, ρ is mass density, U is velocity, e is fluid energy, P is pressure, E is the electric field, B is the magnetic field and subscript s corresponds to species.

Two-Fluid Model: Maxwell's Equations

The two-fluid plasma model consists of a set of fluid equations for the electrons and ions plus the complete Maxwell's equations including displacement current,

$$\partial_t E - \left(\frac{c}{v_{thi}} \right)^2 (\nabla \times B) = - \sum_s \frac{x_0 r_{gi}}{\lambda_d} (n_i U_i - n_e U_e) , \quad (1)$$

$$\partial_t B + (\nabla \times E) = 0 , \quad (2)$$

$$\nabla \cdot B = 0 , \quad (3)$$

$$\nabla \cdot E = \frac{x_0 r_{gi}}{\lambda_d} (n_i - n_e) . \quad (4)$$

Equations (3) and (4) are constraint equations which can be derived from Ampere's law (1) and Faraday's law (2). Consequently (3) and (4) are not solved numerically as they do not provide additional information provided the initial conditions satisfy the constraint equations.

Two-Fluid Model: Fluid Equations

Electrons and ions have separate energy,

$$\partial_t e_s + \nabla \cdot (U_s (e_s + P_s)) = \pm \frac{x_0}{r_{gi}} n_s E \cdot U_s , \quad (5)$$

momentum,

$$\partial_t \rho_s U_s + \nabla \cdot (\rho_s U_s U_s) + \nabla P_s = \pm \frac{x_0}{r_{gi}} n_s (E + U_s \times B) , \quad (6)$$

and continuity equations,

$$\partial_t \rho_s + \nabla \cdot (\rho_s U_s) = 0 , \quad (7)$$

so each species has it's own temperature, velocity and number density. As a result, quasi-neutrality is not assumed and things like electron plasma waves and ion subshocks, and ion current should be observed numerically. This implementation ignores such “non-ideal” effects as collisions and non-isotropic pressures. These terms are dropped to focus on the numerical issues that result from the “ideal” terms that remain.

Two-Fluid Model: Balance Form

This set of equations can be written as three systems of balance laws,

$$\frac{\partial q_e}{\partial t} + \nabla \cdot F_e(q) = \psi_e, \quad (8)$$

for the electron fluid equations,

$$\frac{\partial q_i}{\partial t} + \nabla \cdot F_i(q) = \psi_i, \quad (9)$$

for the ion fluid equations, and

$$\frac{\partial q_{em}}{\partial t} + \nabla \cdot F_{em}(q) = \psi_{em}, \quad (10)$$

for Maxwell's field equations.

Two-Fluid Model: Balance Form

For clarity, these balance laws Eqns.(8)-(10) are given in full form by,

$$\frac{\partial}{\partial t} \begin{pmatrix} \rho_s \\ m_{xs} \\ m_{ys} \\ m_{zs} \\ e_s \end{pmatrix} + \nabla \cdot \begin{pmatrix} \rho_s U_{xs} & \rho_s U_{ys} & \rho_s U_{zs} \\ \rho_s U_{xs} U_{xs} + P_s & \rho_s U_{xs} U_{ys} & \rho_s U_{xs} U_{zs} \\ \rho_s U_{ys} U_{xs} & \rho_s U_{ys} U_{ys} + P_s & \rho_s U_{ys} U_{zs} \\ \rho_s U_{zs} U_{xs} & \rho_s U_{zs} U_{ys} & \rho_s U_{zs} U_{zs} + P_s \\ U_{xs} (e_s + P_s) & U_{ys} (e_s + P_s) & U_{zs} (e_s + P_s) \end{pmatrix} = \pm \begin{pmatrix} 0 \\ \frac{x_0}{r_{gi}} n_s (E_x + U_{ys} B_z - U_{zs} B_y) \\ \frac{x_0}{r_{gi}} n_s (E_y + U_{zs} B_x - U_{xs} B_z) \\ \frac{x_0}{r_{gi}} n_s (E_z + U_{xs} B_y - U_{ys} B_x) \\ \frac{x_0}{r_{gi}} n_s (E_x U_{xs} + E_y U_{ys} + E_z U_{zs}) \end{pmatrix} \quad (11)$$

$$\frac{\partial}{\partial t} \begin{pmatrix} B_x \\ B_y \\ B_z \\ E_x \\ E_y \\ E_z \end{pmatrix} + \nabla \cdot \begin{pmatrix} 0 & E_z & -E_y \\ -E_z & 0 & E_x \\ E_y & -E_x & 0 \\ 0 & -\left(\frac{c}{v_{thi}}\right)^2 B_z & \left(\frac{c}{v_{thi}}\right)^2 B_y \\ \left(\frac{c}{v_{thi}}\right)^2 B_z & 0 & -\left(\frac{c}{v_{thi}}\right)^2 B_x \\ -\left(\frac{c}{v_{thi}}\right)^2 B_y & \left(\frac{c}{v_{thi}}\right)^2 B_x & 0 \end{pmatrix} = \begin{pmatrix} 0 \\ 0 \\ 0 \\ -\frac{x_0}{\lambda_d} \frac{r_{gi}}{\lambda_d} (n_i U_{xi} - n_e U_{xe}) \\ -\frac{x_0}{\lambda_d} \frac{r_{gi}}{\lambda_d} (n_i U_{yi} - n_e U_{ye}) \\ -\frac{x_0}{\lambda_d} \frac{r_{gi}}{\lambda_d} (n_i U_{zi} - n_e U_{ze}) \end{pmatrix} \quad (12)$$

Discontinuous Galerkin Method

Discontinuous Galerkin methods are high order extensions of upwind schemes using a finite element formulation where the elements are discontinuous at cell interfaces.

Details of the method are discussed in [7, 6, 5, 8] and reproduced here for our particular case. The balance law,

$$\frac{\partial q}{\partial t} + \nabla \cdot F = \psi, \quad (13)$$

is multiplied by the set of basis functions $\{v_r\}$ and integrated over the finite volume element K . For second order spatial accuracy the basis set

$\{v_r\} = \{v_0, v_x, v_y\} = \{1, \frac{x-x_{ij}}{\frac{1}{2}\Delta x}, \frac{y-y_{ij}}{\frac{1}{2}\Delta y}\}$ is used. The equation is written,

$$\int \frac{\partial q}{\partial t} v_r dV + \int (\nabla \cdot F) v_r dV = \int \psi v_r dV. \quad (14)$$

Discontinuous Galerkin Method

Integrate by parts to get

$$\int_K \frac{\partial q}{\partial t} v_r dV + \int_{\partial K} (F \cdot n) v_r d\Gamma - \int_K F \cdot (\nabla v_r) dV = \int \psi v_r dV . \quad (15)$$

The discrete conserved variable q is defined as a linear combination of the basis functions inside an element K , $q = q_0 + v_x q_x + v_y q_y$. The integral $\int_K \frac{\partial q}{\partial t} v_r dV = \frac{\partial q_r}{\partial t} C V$ where C is the constant $\frac{1}{V} \int_K v_r^2 dV$ and V is the volume of the element. Using these definitions we get the discrete equation

$$\frac{\partial q_r}{\partial t} C V + \sum_e \sum_l r_l (F \cdot n) v_r \Gamma_e - \sum_m w_m F \cdot (\nabla v_r) V = \sum_m w_m \psi v_r V , \quad (16)$$

when the integrals are replaced by appropriate Gaussian quadratures. Γ_e is the surface area of the cell face in consideration, e refers to an element face, r_l are quadrature points on a face and w_m are quadrature points in the volume.

Discontinuous Galerkin Method

The discrete equations for the second order scheme are

$$\frac{\partial q_0}{\partial t} V + \sum_e \sum_l r_l (F \cdot n) v_0 \Gamma_e = \sum_m w_m \psi v_0 V, \quad (17a)$$

$$\frac{\partial q_x}{\partial t} V + 3 \sum_e \sum_l r_l (F \cdot n) v_x \Gamma_e - 3 \sum_m w_m F \cdot (\nabla v_x) V = 3 \sum_m w_m \psi v_x V, \quad (17b)$$

$$\frac{\partial q_y}{\partial t} V + 3 \sum_e \sum_l r_l (F \cdot n) v_y \Gamma_e - 3 \sum_m w_m F \cdot (\nabla v_y) V = 3 \sum_m w_m \psi v_y V. \quad (17c)$$

The derivatives of the basis functions can be calculated analytically since the polynomial basis functions are known. The discontinuous Galerkin method is applied to each balance law (8)(9)(10) at every time step. In [7] TVD Runge-Kutta time integration is suggested, though standard Runge-Kutta methods work well. In this paper we use a 3rd order TVD Runge-Kutta a scheme as in [7].

Limiters

As in high-resolution methods, the q are first transformed to characteristic variables g where $g = L q$ and L is the left eigenvector matrix of the flux Jacobian calculated from q_0 . The left eigenvector matrix is also applied to the differences $L (q_0^{i+1} - q_0^i) = \Delta^+ g_0$ and $L (q_0^i - q_0^{i-1}) = \Delta^- g_0$. Limiting is performed directly on transformed variables and then the solution is immediately transformed back to determine the limited form of q_x ,

$$q_x = L^{-1} m (g_x, \Delta^+ g_0, \Delta^- g_0) \quad (18)$$

where m is the minmod limiter defined by

$$m(a, b, c) = \begin{cases} \max(a, b, c) & \text{if } \text{sign}(a) = \text{sign}(b) = \text{sign}(c) = - \\ \min(a, b, c) & \text{if } \text{sign}(a) = \text{sign}(b) = \text{sign}(c) = + \\ 0 & \text{otherwise} \end{cases} \quad (19)$$

Limiters

The minmod limiter Eqn. (19) is used for each of the fluid equations Eqn.(8)(9) while if the simulation is 2D a modified minmod limiter is used on Maxwell's equations Eqn.(10) so that divergence errors in the B field are reduced. $\nabla \cdot B$ errors have been problematic for high-resolution methods. Using the discontinuous Galerkin method the $\nabla \cdot B$ errors can be reduced simply by eliminating limiters from the Maxwell algorithm altogether or using the TVBM limiters described in [7]. The TVBM limiter \bar{m} is

$$\bar{m}(a, b, c) = \begin{cases} a & \text{if } a < M \Delta x^2 \\ m(a, b, c) & \text{otherwise} \end{cases} . \quad (20)$$

Where M is a constant.

Magnetic Reconnection: GEM Challenge

In ideal MHD the fluid is frozen to the magnetic field lines and so field lines cannot reconnect without some non-ideal term. Resistivity allows field lines to reconnect though much slower than the fast reconnection that is observed in the earth's magnetotail, in solar flares or in sawtooth collapse in tokamaks[2]. This fast reconnection requires at least the addition of the Hall term and means that magnetic reconnection can be simulated using the two fluid plasma model.

The GEM challenge magnetic reconnection problem is non-dimensionalized as in [10] where lengths are normalized by the ion inertial length $d = c/w_{pi} = c \left(\frac{e^2 n_0}{\epsilon_0 m_i} \right)^{-\frac{1}{2}}$ time is non-dimensionalized by the ion-cyclotron time $\frac{m_i}{e B_0}$ where B_0 is the magnetic field at infinity. The velocities are normalized by the Alfvén velocity $V_a = \left(\frac{B_0^2}{\mu_0 m_i n_0} \right)^{\frac{1}{2}}$. The current density is non-dimensionalized by $J_0 = \frac{B_0 w_{pi}}{\mu_0 c}$ and E by $E_0 = V_a B_0$. The domain is $[-\frac{1}{2}L_x d, \frac{1}{2}L_x d] \times [-\frac{1}{2}L_y d, \frac{1}{2}L_y d]$ with $L_x = 25.6$ and $L_y = 12.8$. Non-reflecting boundary conditions are used on the y boundaries while periodic boundary conditions are used on the x boundaries. In this simulation $\lambda = 0.5 d$ and the ion to electron mass ratio is taken to be 25, the specific heat ratio $\gamma = \frac{5}{3}$ for both electrons and ions and $\frac{V_a}{c} = \frac{1}{100}$.

Magnetic Reconnection: GEM Challenge

The initial number densities are given by,

$$n_e = n_i = n_0 \left(\frac{1}{5} + \operatorname{sech}^2 \left(\frac{y}{\lambda} \right) \right). \quad (21)$$

The electron pressure is $P_e = \frac{1}{12\mu_0} B_0^2 n_e$ and the ion pressure is $P_i = \frac{5}{12\mu_0} B_0^2 n_i$. The magnetic field is given by

$$B_x = B_0 \tanh \left(\frac{y}{\lambda} \right) + \frac{B_0}{10} \frac{\pi}{L_x} \cos \left(\frac{2\pi x}{L_x} \right) \sin \left(\frac{\pi y}{L_y} \right) \quad (22)$$

$$B_y = \frac{B_0}{10} \left(\frac{2\pi}{L_x} \right) \sin \left(\frac{2\pi x}{L_x} \right) \cos \left(\frac{\pi y}{L_y} \right) \quad (23)$$

The initial electron current J_{ze} is,

$$J_{ze} = -\frac{\mu_0 B_0}{\lambda} \operatorname{sech}^2 \left(\frac{y}{\lambda} \right). \quad (24)$$

Magnetic Reconnection: GEM Challenge

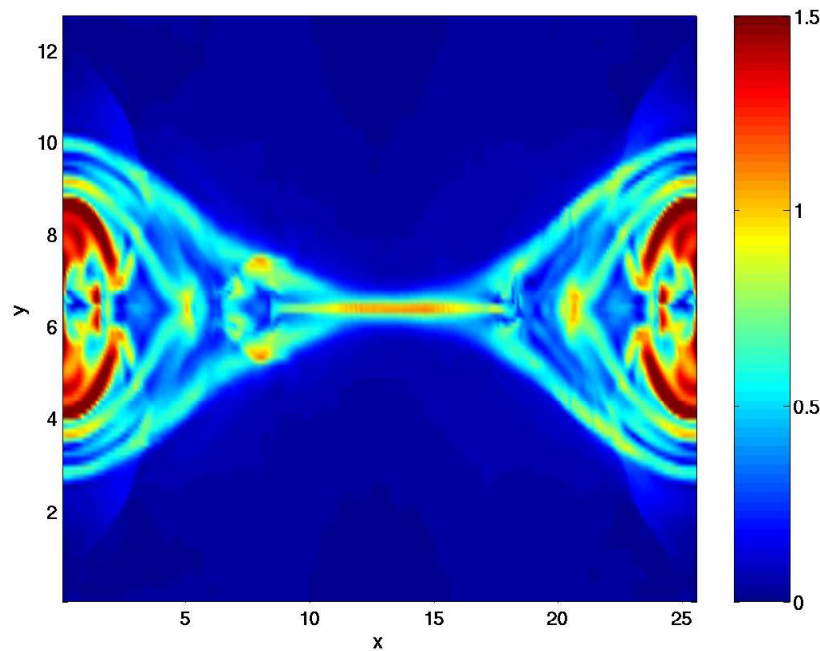


Figure 1: Magnitude of electron current in the GEM challenge problem after $t = 25/\omega_{ci}$. The current layer thins in the center of the domain and small shock waves are visible at the corners of the plot. This problem is highly susceptible to round off errors and numerical experiments have shown that increasing the accuracy of our floating point numbers from 64 bit to 96 bit helps to symmetrize the solution.

Magnetic Reconnection: GEM Challenge

BIRN ET AL.: GEM RECONNECTION CHALLENGE

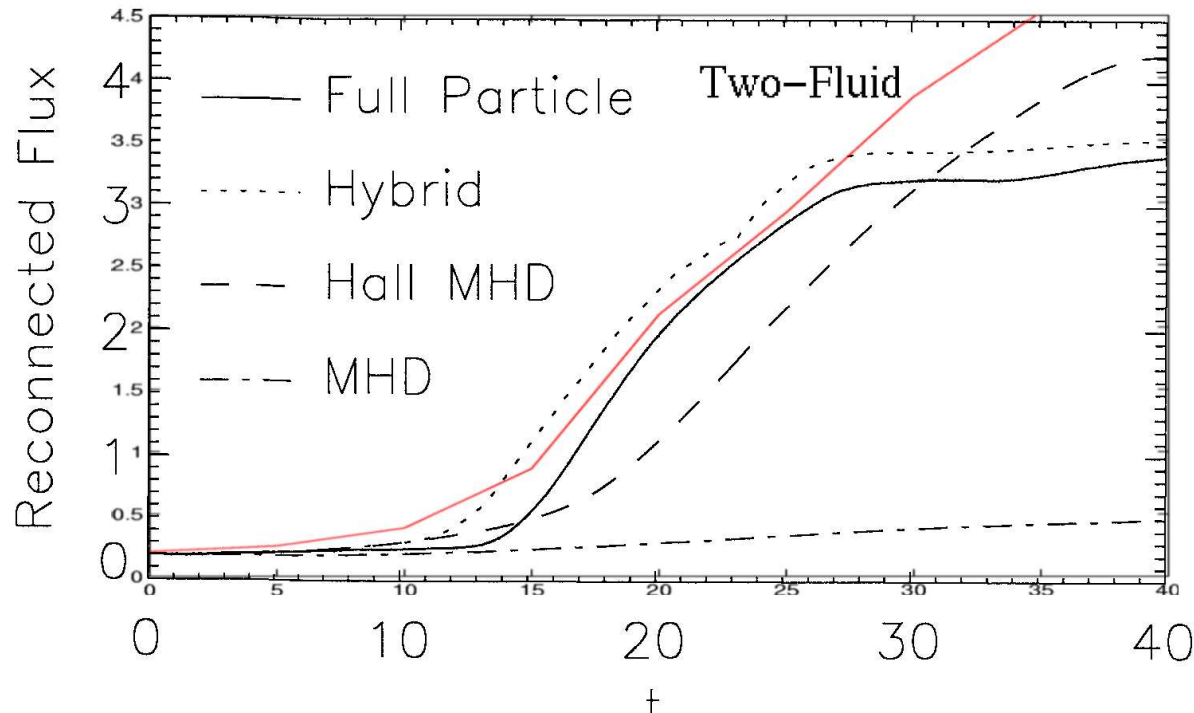


Figure 2: Plot of reconnected magnetic flux vs time in units of inverse ω_{ci} for several published solutions and the two-fluid solution calculated by the authors.

Magnetic Reconnection

In Fig. 2 the two-fluid solution is compared to solutions published in the GEM challenge papers [10]. The two-fluid solution shows good agreement with published solutions except that flux continues to reconnect in the two-fluid solution after it has saturated in the published solutions. This is believed to be caused by the fact that the two-fluid solution uses open y boundaries so fluid and magnetic field lines continue to flow in from the y boundaries. In the published results, conducting walls were used on the y boundaries which prevents fluid and flux from entering the domain so the solution saturates.

Theta Pinch

The theta pinch is a confinement concept where an azimuthal current is supported by an axial magnetic field to confine a plasma. In this simulation strong shear in the electron current layer drives an instability in an equilibrium configuration. This sort of phenomena is not observed in MHD simulations of current layers because the current equation in MHD (Ohm's law) lacks the convective derivative and pressure term. Preliminary results suggest that increased resolution or a higher order discontinuous Galerkin method will help to improve the solutions in figures 3 and 4 as significant dissipation of the thin current sheet is observed using the second order discontinuous Galerkin method.

Theta Pinch

In the theta pinch equilibrium we set

- Initial electron current

$$J_{ze} = 10 \operatorname{sech}^2(a(r - r_0)) \hat{\theta} \quad (25)$$

- Initial pressure and number density.

$$P = P_0 - \frac{1}{2} B_z^2 \quad \text{where} \quad P_0 = \frac{1}{2} (1 + \alpha) \quad (26)$$

With $P_i = P_e = \frac{1}{2} P$ and $n_i = n_e = \frac{P}{P_0}$.

- Initial magnetic field

$$B_z = -\frac{1}{2} \frac{e^{2a(r-r_0)} - 1}{(e^{2a(r-r_0)} + 1)} - B_0 \quad \text{where} \quad B_0 = -\frac{1}{2} \frac{e^{-2ar_0} - 1}{(e^{-2ar_0} + 1)} \quad (27)$$

Where $a = 100$, $r_0 = 0.25$, $\alpha = \frac{1}{10}$ on the domain $[-0.5x_0, 0.5x_0] \times [-0.5x_0, 0.5x_0]$

with non-reflecting boundary conditions. In this simulation characteristic parameters are

$$\frac{r_{gi}}{x_0} = \frac{1}{10}, \quad \frac{\lambda_d}{x_0} = \frac{2}{1000}, \quad \frac{v_{thi}}{c} = \frac{1}{100} \quad \text{and} \quad \frac{m_i}{m_e} = 1836 \text{ or } 25.$$

Theta Pinch

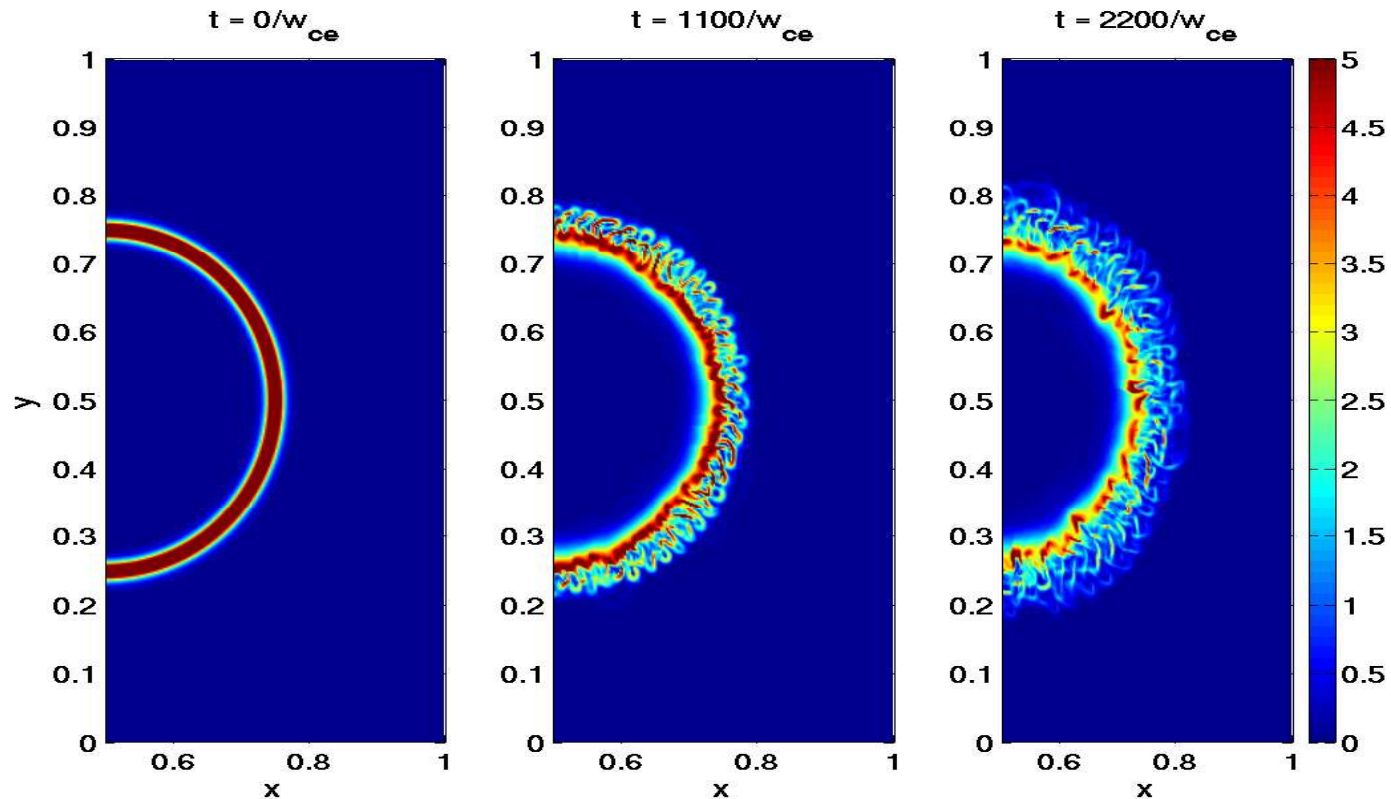


Figure 3: Plot of total electron current in the theta pinch problem using an ion to electron mass ratio of 1836. The loops form when the electron fluid gyrates around a magnetic field line

Theta Pinch

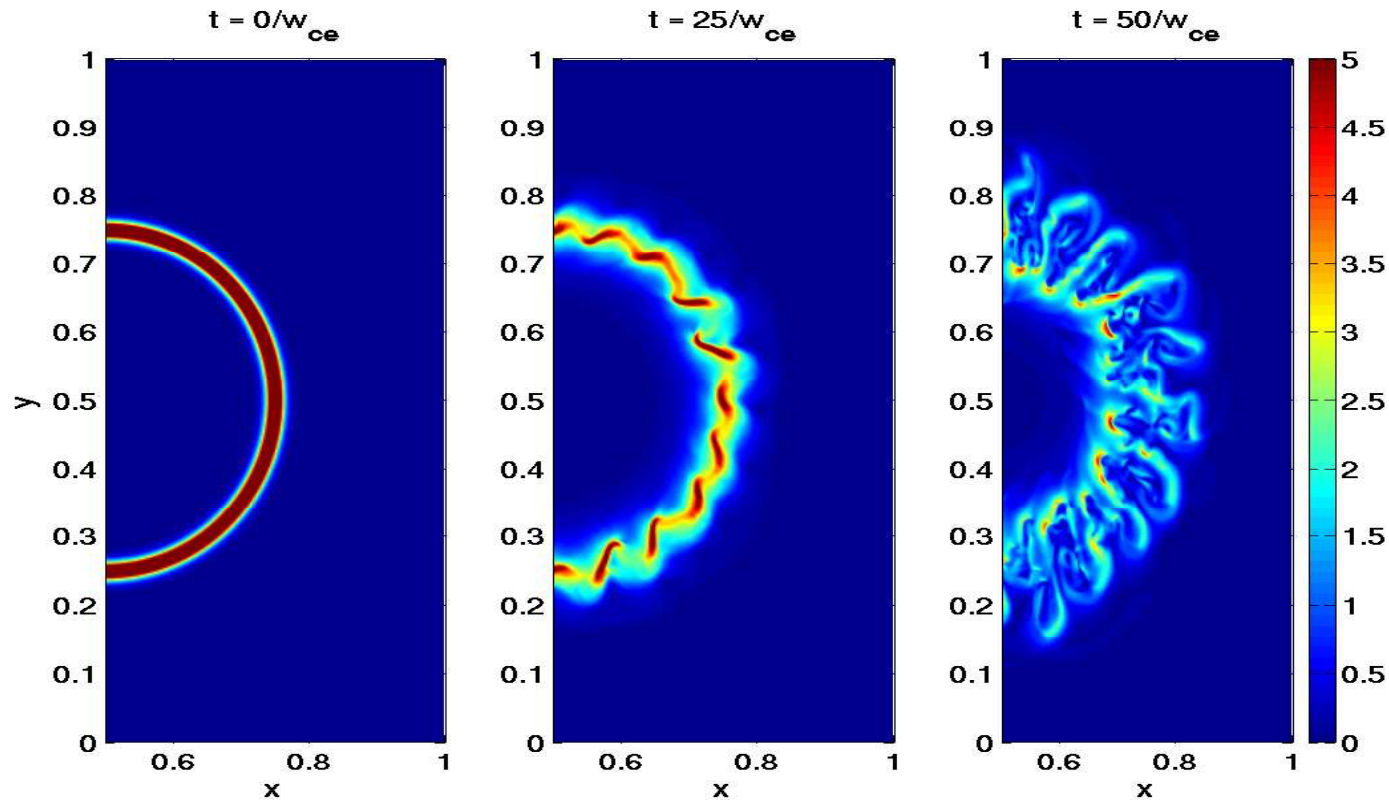


Figure 4: Plot of the total electron current in the theta pinch problem using an ion to electron mass ratio of 25. The extra momentum that the electrons carry increases the size of the loops compared to the previous figure.

Conclusion

A discontinuous Galerkin method for the two-fluid plasma model has been described. The algorithm uses a second order spatial discretization and a 3rd order TVD Runge-Kutta time stepping scheme. TVDM limiters are used on the electron and ion fluid equations while TVBM limiters are used for Maxwell's equations to help maintain the $\nabla \cdot B$ condition. The algorithm produces solutions to the GEM challenge magnetic reconnection problem that agree with published solutions. The algorithm has been tested on a theta-pinch equilibrium where plasma instabilities quickly develop producing turbulence. The algorithm should be easy to extend to 3 dimensions and complex geometries as well as to higher order accuracy.

References

- [1] A. Bhattacharjee, *Center for magnetic reconnection studies: Present status, future plans*, PSACI PAC Presentation, Princeton, June 2003.
- [2] Dieter Biskamp, *Magnetic reconnection in plasmas*, Cambridge University Press, 2000.
- [3] J.A. Breslau and S.C. Jardin, *A parallel algorithm for global magnetic reconnection studies*, Computer Physics Communications **151** (2003), 8–24.
- [4] L. Chacon and D.A. Knoll, *A 2d high-beta hall mhd implicit nonlinear solver*, Journal of Computational Physics **188** (2003), 573–592.
- [5] Bernardo Cockburn, Suchung Hou, and Chi-Wang Shu, *The runge-kutta local projection discontinuous galerkin finite element method for conservation laws iv: Multidimensional case*, Mathematics of Computation **54** (1990), 545–581.
- [6] Bernardo Cockburn, San-Yih Lin, and Chi-Wang Shu, *Tvb runge-kutta local projection discontinuous galerkin finite element method for conservation laws iii: One-dimensional systems*, Journal of Computational Physics **84** (1989), 90–113.
- [7] Bernardo Cockburn and Chi-Wang Shu, *Tvb runge-kutta local projection discontinuous galerkin finite element method for conservation laws ii: General framework*, Mathematics of Computation **52** (1989), 411–435.
- [8] _____, *The runge-kutta discontinuous galerkin method for conservation laws v: Multidimensional systems*, Journal of Computational Physics **141** (1998), 199–224.

- [9] C.R. Sovinec et. al., *Nonlinear magnetohydrodynamics simulation using high-order finite elements*, Journal of Computational Physics **195** (2004), 355–386.
- [10] J. Birn et. al., *Geospace environmental modeling (gem) magnetic reconnection challenge*, Journal of Geophysical Research **106** (2001), no. A3, 3715–3719.
- [11] W. Park et. al., *Plasma simulation studies using multilevel physics models*, Physics of Plasmas **6** (1999), no. 5, 1796–1803.
- [12] D.S. Harned and Z. Mikic, *Accurate semi-implicit treatment of the hall effect in magnetohydrodynamic computations*, Journal of Computational Physics **83** (1989), 1–15.
- [13] Joseph D. Huba, *Hall magnetohydrodynamics - a tutorial*, Space Plasma Simulation (M. Scholer J. Buchner, C.T. Dunn, ed.), Springer, 2003, pp. 166–192.
- [14] A. Ishida, H. Momota, and L.C. Steinhauer, *Variational formulation for a multifluid flowing plasma with application to the internal tilt mode of a field-reversed configuration*, Physics of Fluids **31** (1988), no. 10, 3024–3034.
- [15] U. Shumlak and J. Loverich, *Approximate riemann solver for the two-fluid plasma model*, Journal of Computational Physics **187** (2003), 620–638.
- [16] Toshiko Tajima, *Computational plasma physics: With applications to fusion and astrophysics*, Addison-Wesley, 1989.